HHS Public Access

Author manuscript

Mol Microbiol. Author manuscript; available in PMC 2015 April 13.

Published in final edited form as:

Mol Microbiol. 2010 March ; 75(6): 1563–1576. doi:10.1111/j.1365-2958.2010.07078.x.

Inactivation of a putative flagellar motor switch protein FliG1 prevents *Borrelia burgdorferi* from swimming in highly viscous media and blocks its infectivity

Chunhao Li[1,*], **Hongbin Xu**[1], **Kai Zhang**[1], and **Fang Ting Liang**[2]

[1]Department of Oral Biology, the State University of New York at Buffalo, NY 14214, USA

[2]Department of Pathobiological Sciences, Louisiana State University, Baton Rouge, LA 70803, USA

Summary

The flagellar motor switch complex protein FliG plays an essential role in flagella biosynthesis and motility. In most motile bacteria, only one *fliG* homologue is present in the genome. However, several spirochete species have two putative *fliG* genes (referred to as *fliG1* and *fliG2*) and their roles in flagella assembly and motility remain unknown. In this report, the Lyme disease spirochete *Borrelia burgdorferi* was used as a genetic model to investigate the roles of these two *fliG* homologues. It was found that *fliG2* encodes a typical motor switch complex protein that is required for the flagellation and motility of *B. burgdorferi*. In contrast, the function of *fliG1* is quite unique. Disruption of *fliG1* did not affect flagellation and the mutant was still motile but failed to translate in highly viscous media. GFP-fusion and motion tracking analyses revealed that FliG1 asymmetrically locates at one end of cells and the loss of *fliG1* somehow impacted one bundle of flagella rotation. In addition, animal studies demonstrated that the *fliG1*− mutant was quickly cleared after inoculation into the murine host, which highlights the importance of the ability to swim in highly viscous media in the infectivity of *B. burgdorferi* and probably other pathogenic spirochetes.

Introduction

Spirochetes are a group of medically and ecologically important but poorly understood bacteria. Spirochetes can be classified into free-living, symbiotic and pathogenic groups based on their habitats and pathogenicity (Charon and Goldstein, 2002; Rosa *et al.*, 2005). Pathogenic spirochetes can cause a variety of human and animal diseases, some of which are quite prevalent and can have grave consequences. For example, Lyme disease, caused by the spirochete *Borrelia burgdorferi*, is the most prevalent vector-borne disease in the USA (Steere *et al.*, 2004; Rosa *et al.*, 2005). Many *Leptospira* species cause leptospirosis. This

*For correspondence. cli9@buffalo.edu; Tel. (+1) 716 829 6014; Fax (+1) 716 829 3942.

Supporting information

Additional supporting information may be found in the online version of this article.

Please note: Wiley-Blackwell are not responsible for the content or functionality of any supporting materials supplied by the authors. Any queries (other than missing material) should be directed to the corresponding author for the article.

potentially fatal water-borne zoonosis has many possible clinical manifestations and occurs worldwide (Levett, 2001; Mcbride *et al.*, 2005). *Treponema pallidum* causes the dreaded sexually transmitted disease, syphilis, which is a major disease in developing countries worldwide (Weinstock *et al.*, 1998; Chen *et al.*, 2007). *Brachyspira* spp. can cause both human and animal gastrointestinal diseases (Mikosza and Hampson, 2001). The symbiotic spirochetes that dwell in the hind-guts of termites provide their insect host with essential nutrients via acetogenesis and nitrogen fixation, which is one of the most striking examples of the extraordinary biodiversity achieved by spirochetes (Leadbetter *et al.*, 1999; Warnecke *et al.*, 2007).

Spirochetes are very diverse but they constitute a monophlytic group of bacteria that share some common characteristics: unique helical or planar wave-like cell morphology and an unusual means of motility (Holt, 1978; Paster and Dewhirst, 2000). Spirochetes have a protoplasmic cell cylinder surrounded by an outer membrane sheath. In the periplasm, between the peptidoglycan layer and the outer membrane, are periplasmic flagella (PFs). In many spirochete species, PFs are long enough to overlap in the centre of the cell with those extending from the opposite ends. The number of PFs at each end varies from species to species (Charon and Goldstein, 2002). PFs are clearly the spirochetes' organelles of motility since mutations that inhibited the synthesis of PFs resulted in non-motile phenotype (Motaleb *et al.*, 2000; Li *et al.*, 2008; Sal *et al.*, 2008). Such unique cell morphology and structure give spirochetes an unusual means of motility: spirochetes can swim in a highly viscous, gel-like medium, such as that found in connective tissue, that inhibits the motility of most other motile bacteria (Greenberg and Canale-Parola, 1977a; Berg and Turner, 1979; Charon and Goldstein, 2002). In fact, the speed of spirochetes actually accelerates as viscosity increases. For example, the speed of *Treponema denticola* increases from less than 1 μm s^{-1} in liquid media to 19 μm s^{-1} in the presence of 1% methylcellulose (Ruby and Charon, 1998).

It is widely believed that this unique means of motility is essential for the pathogenesis of spirochetes, e.g. it may empower the spirochetes to penetrate into tissues, and help these organisms to escape from the innate immune response and rapidly disseminate in mammalian hosts (Kimsey and Spielman, 1990; Lux *et al.*, 2000; Charon and Goldstein, 2002). Consistently, clinical evidence has shown that these pathogenic spirochetes are highly invasive in hosts. For example, *B. burgdorferi* can be recovered from the vitreous humour of the eye, brain tissues, endomyocardial tissue and other tissues of Lyme disease patients (Stanek *et al.*, 1990; Kuiper *et al.*, 1994; Nocton *et al.*, 1996). *Leptospira interrogans* can be isolated from cerebrospinal fluid and the kidneys of patients (Brown *et al.*, 2003; Palaniappan *et al.*, 2007). However, due to the difficulty in obtaining the mutants that only fail to swim in highly viscous media, the biology about this unique means of motility and its role in the infections are poorly understood.

Among these pathogenic spirochetes, *B. burgdorferi* is one of the best understood spirochetes and one for which genetic tools have rapidly evolved in the past few years (Rosa *et al.*, 2005). For example, genetic targeting mutagenesis mediated by allelic exchange and a whole genome transposon mutagenesis were successfully developed (Samuels *et al.*, 1994; 1995; Stewart *et al.*, 2004; Botkin *et al.*, 2006). In addition, multiple antibiotic selection

markers and a number of shuttle plasmids have been developed to inactivate genes, complement inactivated genes or express green fluorescent protein (GFP) and luciferase in *B. burgdorferi* (Eggers *et al.*, 2002; Elias *et al.*, 2003; Blevins *et al.*, 2007). Most importantly, animal models of Lyme disease have been well established and extensively used to study the pathogenesis of *B. burgdorferi* (Masuzawa *et al.*, 1992; Barthold, 1995). Theses advantages make this spirochete an ideal model to study the unique means of motility and its role in the process of disease.

The genome of *B. burgdorferi* encodes 59 motility and chemotaxis genes, which constitutes approximately 5% of its total genes (Fraser *et al.*, 1997; Li *et al.*, 2000; Charon and Goldstein, 2002). In our recent studies, several genes involved in motility and chemotaxis have been studied, which include two flagella genes (*flaB* and *flgE*) and three chemotaxis genes (*cheA1*, *cheA2* and *cheX*). The results show that the *flaB* and *flgE* genes are essential for the flagella synthesis and motility, and the *cheA2* and *cheX* genes are critical for the chemotaxis of *B. burgdorferi* (Motaleb *et al.*, 2000; 2005; Li *et al.*, 2002; Sal *et al.*, 2008). Following previous studies, more motility and chemotaxis genes have recently been inactivated. Among these genes, *fliG*, a gene encoding a flagellar motor switch complex protein, plays an essential role in flagella assembly and motility in enteric bacteria and other flagellated bacteria (Lloyd *et al.*, 1996). For instance, the *fliG* null mutants of *Escherichia coli* and *Salmonella enterica* are aflagellated and non-motile. In most motile bacteria, only one *fliG* is present in their genomes. However, in several spirochete species including *B. burgdorferi*, there are two *fliG* homologues (referred to as *fliG1* and *fliG2*). The functions of these two *fliG* genes remain unknown. In this report, these two genes were inactivated and their roles in flagella assembly and motility were evaluated. In addition, the role of motility in the virulence of *B. burgdorferi* was investigated by analysis of the *fliG1* mutant in the mouse model of Lyme disease.

Results

Sequence alignment reveals that FliG2, but not FliG1, is a typical motor switch complex protein

As mentioned above, FliG proteins play a key role in bacterial flagella biosynthesis and motility (Irikura *et al.*, 1993; Lloyd *et al.*, 1996). In most flagellated bacteria, there is only one *fliG* gene. However, there are two *fliG* genes in the sequenced spirochete genomes. In *B. burgdorferi*, *fliG1* (*BB0221*) and *fliG2* (*BB0290*) encode a 405-amino-acid protein with a predicted molecular weight of 47.5 kDa and a 344-amino-acid protein with a predicted molecular weight of 34.3 kDa, respectively (Fraser *et al.*, 1997). BLAST analysis showed that FliG2 shares a 32% identity and a 55% similarity to *E. coli* FliG, and FliG1 shares a 17% identity and a 45% similarity to that of *E. coli*. Prior to this study, it was unknown whether these two genes had redundant or unique functions in flagella assembly and motility.

Previous functional and structural analyses have shown that the C-terminal sequences of FliG proteins are extremely conserved and contain 20 key residues that are required for their functions or structures (Lloyd *et al.*, 1999). To reveal the potential roles of FliG1 and FliG2, the C-terminal sequences of these two proteins were aligned with their counterparts from

other bacteria. As shown in Fig. 1, the C-terminus of FliG2 is well conserved, and it contains all key residues. In contrast, although the C-terminus of FliG1 shares certain identity to its counterparts, it lacks seven key residues. This comparison suggests that FliG2 is a typical motor switch protein that may have the similar function as its counterparts, whereas FliG1 is an atypical motor switch protein and its function may be unique.

Generations of *fliG1*− and *fliG2*− mutants

To disclose the roles of *fliG1* and *fliG2*, these two genes were inactivated by targeted mutagenesis as described in Fig. 2. For *fliG1*, nine kanamycin-resistant colonies appeared 17 days after plating, and for *fliG2*, 11 kanamycin-resistant colonies appeared 24 days after plating. The time required for the appearance of these two mutant colonies is considerably longer than the time required for the appearance of colonies of the wild type (10–14 days).A similar phenotype was observed in the *flaB* and *flgE* mutants of *B. burgdorferi* (Motaleb *et al.*, 2000; Sal *et al.*, 2008). For each mutant, one of clones, which was, respectively, referred to as *fliG1*− or *fliG2*−, was selected for detailed characterization. A PCR analysis described before (Motaleb *et al.*, 2000; Sal *et al.*, 2008) showed the *kan*-resistant cassette was inserted within and transcribed as the same direction of *fliG1* or *fliG2* as expected (data not shown). Western blot analysis with an antiserum against FliG1 or FliG2 further confirmed that the cognate gene products were, respectively, inhibited in the mutants. As shown in Fig. 3B and C, a single band of 48 kDa or 35 kDa protein product was detected in the wild type, but they were absent in *fliG1*− or *fliG2*−. Taken together, these results demonstrated that *fliG1* and *fliG2* were expressed and the cognate gene product was disrupted in the respective mutant due to the targeted mutagenesis.

FliG2, but not FliG1, is essential for flagella synthesis

In enteric bacteria, the *fliG* genes are essential for flagella assembly and motility. The null *fliG* mutants are aflagellated and non-motile. To detect the influence of *fliG1* and *fliG2* on the synthesis of PFs, the mutants were analysed by electron microscopy. In the micrographs of outer membrane disrupted cells, two bundles of PFs were observed at two ends of the wild-type and *fliG1*− cells. However, such structures were absent in the *fliG2*− cells (Fig. 4, top panel). In the micrographs of thin sections, there were 9–11 PFs present in the periplasm of the wild type and *fliG1*−. In contrast, the *fliG2*− mutant completely lacked PFs (Fig. 4, low panel). Western blot further confirmed that two flagellar filament proteins FlaA and FlaB were absent in *fliG2*− but present in *fliG1*− (Fig. 3A). These results demonstrated that FliG2 is a typical motor switch protein that is essential for the flagella synthesis. In contrast, FliG1 was shown as an atypical motor switch protein since it was not critical for the flagella synthesis of *B. burgdorferi*.

The *fliG2*− mutant is totally non-motile whereas the *fliG1*− mutant only fails to translate in a highly viscous medium

The impact of *fliG1* and *fliG2* on the motility of *B. burgdorferi* was evaluated by different methods, which include microscopic observation, swarm plate assay and bacterial tracking analysis (Bakker *et al.*, 2006; Motaleb *et al.*, 2007; Li *et al.*, 2008; Sal *et al.*, 2008). Dark-field microscopic analysis revealed that the *fliG2*− mutant cells were rod-shaped and often

grew in chains, and were completely non-motile (data not shown). The observed phenotype is the same as previously reported *B. burgdorferi* aflagellated mutants (Motaleb *et al.*, 2000; Sal *et al.*, 2008). In contrast to the phenotype of *fliG2*−, the *fliG1*−mutant did not have significant changes in terms of cell morphology and swimming behaviour: the mutant still had a flat-wave morphology (data not shown) and the mutant was still motile in liquid BSK-II medium (Goldstein *et al.*, 1994; Li *et al.*, 2002).

Swarm plate assays further confirmed that *fliG2*− is non-motile. Interestingly, the swarm plate assays revealed that the motility of *fliG1*− was partially decreased, and the complemented strain *fliG1*$^{-/+}$ restored the full motility as the wild type (Fig. 5), indicating that inactivation of *fliG1* somehow reduced the ability of the mutant to swim on soft agarose plates. To quantitatively measure the motility, the mutants were analysed by a previously developed computer-based bacterial tracking system (Li *et al.*, 2002; Bakker *et al.*, 2006). Previous studies have revealed that spirochetes, including *B. burgdorferi*, do not translate very well in low viscous media such as BSK-II, and their swimming ability (velocity) is accelerated in highly viscous media such as 1% methylcellulose. As expected, both the wild-type and the *fliG1*− mutant cells were unable to efficiently displace in BSK-II medium and their velocities were less than 1 μm s^{-1} (Table 1). In 1% methylcellulose medium, the velocity of wild-type cells (Video S1) increased to approximately 10 μm s^{-1} whereas the *fliG1*−mutant completely failed to displace (Video S2, and Table 1). Taken together, these results showed that the inactivation of *fliG1* somehow abrogated the ability of spirochete cells to displace in a highly viscous medium.

One end of the *fliG1*− mutant cells failed to gyrate

Previous studies have shown that two bundles of PFs, one at each end of the spirochete cells, can rotate and generate torque that leads to swimming. The co-ordinated rotation of two bundles of PFs is essential for the motility of spirochetes (Goldstein *et al.*, 1994; Charon and Goldstein, 2002; Li *et al.*, 2002). To further disclose the mechanism involved in the above observed phenotype, the *fliG1*− mutant cells in BSK-II medium were videotaped under high-magnification dark-field microscopy (100×) as previously described (Li *et al.*, 2002). This method allows us to closely observe the motion at both ends of the cells. As shown in Video S3, for the wild-type cells, both ends could actively rotate and took turns being a leading end. However, for the *fliG1*− mutant cells, only one end was actively rotating and the other end failed to be a leading end (Video S4), suggesting that the flagella motors at one end of the cells may be paralysed due to the inactivation of *fliG1*.

FliG1 locates at one end whereas FliG2 resides at two ends of *B. burgdorferi* cells

The above studies showed that the inactivation of *fliG1* only altered the rotation of PFs at one end of cells, implying that the FliG1 protein may locate at one end of the cells. To address this speculation, GFP-fusion technique was applied to determine the cellular location of FliG1. A vector that expresses GFP–FliG1 fusion protein was constructed (Fig. 6A). In our previous studies, the strength of different promoters identified in *B. burgdorferi* was evaluated by GFP reporter assay, and we found that the *flgB* promoter could control the expression of GFP at moderate levels (Yang and Li, 2009). As shown in Fig. 6B, the GFP–FliG1 fusion protein was successfully expressed in the *fliG1*− mutant. Some degraded

products were detected by monoclonal GFP antibody, which is commonly observed in this study (Sourjik and Berg, 2000). However, such degraded products could not be detected using FliG1 antiserum as a probe (data not shown), indicating that the degradation occurred at the portion of GFP. In addition, the strain expressing GFP–FliG1 restored the ability to swim in 1% methylcellulose, indicating GFP–FliG1 was able to substitute the function of FliG1 (data not shown). Under fluorescent microscopy, we found that GFP–FliG1 only located at one end of the cells (Fig. 6D). This pattern was not observed in the control that only expresses GFP (Fig. 6C). This result indicated that FliG1 asymmetrically locates at one end of *B. burgdorferi* cells.

The same method was used to determine the cellular location of FliG2. However, neither FliG2 nor GFP–FliG2 could complement *fliG2*− (data not shown). Immunofluorescence microscopy has been extensively applied to investigate protein cellular locations, including bacterial flagella and chemotaxis proteins (Sourjik and Berg, 2000). As such, this method was conducted to localize FliG2. For this assay, we used a primary antibody specifically reacted with FliG2 and a secondary antibody coupled with Texas red. As shown in Fig. 7, brightest spots were observed at the two poles of the wild-type cells but not in the *fliG2*− mutant, demonstrating that FliG2 symmetrically resides at both ends of *B. burgdorferi* cells.

The *fliG1*− mutant is unable to survive in the mammalian host

The motility of spirochetes is accelerated in highly viscous media such as connective tissues that either slow down or stop most externally flagellated bacteria (Greenberg and Canale-Parola, 1977a,b; Charon and Goldstein, 2002). It is believed that such ability is essential for the infections of spirochetes (Kimsey and Spielman, 1990; Lux *et al.*, 2000). Above studies showed that the *fliG1*− mutant failed to swim in a highly viscous medium. Thus, this mutant can be used to test whether the ability to swim in highly viscous media is essential for the infection. However, the above mutant was constructed in an avirulent background, and cannot be tested in animal studies. To solve this problem, the mutant was re-constructed in B31-A3, a low passage virulent strain (Elias *et al.*, 2002; Grimm *et al.*, 2004). Three positive clones were obtained, which were confirmed by PCR and Western blot analyses as described above (data not shown), and two of them had the full plasmid content of B31-A3. One clone, *vfliG1*−, was further complemented. Although 19 transformants were obtained, only one clone, *vfliG1*$^{-/+}$, had the full plasmid content as its parental strain, B31-A3 (Fig. S1). Microscopic observation, swarm plate assay and bacterial tracking analysis confirmed that these two newly constructed strains exhibited the similar phenotype as their counterparts derived from the B31A strain (data not shown).

The wild-type B31-A3, the mutant *vfliG1*− and the complemented strain *vfliG1*$^{-/+}$ were inoculated into immunocompetent BALB/c mice. Four weeks later, heart, tibiotarsal joint and skin specimens were aseptically collected for spirochete culture. The presence of spirochete cells were used to evaluate the infectivity of these three strains. As shown in Table 2, the wild-type and the complemented strain infected all inoculated mice. In contrast, the mutant could not be recovered from any tissue of inoculated mice, indicating that the ability to swim in highly viscous media is essential for mammalian infection.

After being deposited in skin following tick bites, *B. burgdorferi* must traverse the intercellular matrix, penetrate the vascular endothelial cell lining and become haematogenous (Kimsey and Spielman, 1990; Charon and Goldstein, 2002). It is believed that the ability to swim in highly viscous media, such as connective tissues, facilitates the accomplishment of the above process and consequently helps the spirochete to escape from host innate immunity and establish systematic infection. Thus, the failure of the *vfliG1*− mutant to establish a systemic infection in immunocompetent mice could be due to the loss of motility, which may be required for dissemination and/or for evasion of both innate and adaptive immune responses. To investigate these issues, the three strains were inoculated into SCID mice. As shown in Table 3, the *vfliG1*− mutant was cleared from all of the inoculation sites within 24 h. In contrast, the wild-type B31-A3 and *vfliG1*$^{-/+}$ were recovered from each of the inoculation sites at all time points, indicating that the motility is required for the basic survival of *B. burgdorferi* in the murine host.

Discussion

The flagellar motor switch protein FliG plays a very important role in the flagella biosynthesis and motility (Irikura *et al.*, 1993; Lloyd *et al.*, 1996). The FliG proteins are well conserved among different bacteria and their functions and structures have been well studied in the enteric bacteria such as *E. coli* (Lloyd *et al.*, 1999; Brown *et al.*, 2002). Except for spirochetes, only one copy of the *fliG* gene has been identified in most sequenced bacterial genomes. Interestingly, there are two homologues of *fliG* genes in the sequenced spirochete genomes such as *T. denticola*, *T. pallidum* and *L. interrogans* (Fraser *et al.*, 1997; 1998; Ren *et al.*, 2003; Seshadri *et al.*, 2004). The functions of these two *fliG* genes remain unknown. In this report, different approaches have been applied to elucidate the functions of these two FliG proteins in *B. burgdorferi*. First, the sequence alignment showed that FliG2 shares higher identity (32%) with its counterparts from the enteric bacteria than FliG1 (17%); FliG2 contains all the key residues that are required for its function and structure, but FliG1 lacks seven key residues (Fig. 1). Second, the genetic studies demonstrated that the *fliG2*−mutant shares the similar phenotype as its counterparts of the enteric bacteria: the mutant is aflagellated and non-motile (Irikura *et al.*, 1993). In contrast, the phenotype of the *fliG1*− mutant is quite different: the mutant still synthesized flagella and only failed to translate in highly viscous medium such as 1% methylcellulose (Figs 3–5 and Table 1). Taken together, these studies indicated that FliG2 is a typical motor switch protein that is essential for the flagella synthesis and motility, and FliG1 is an atypical motor switch protein since it is not required for flagella synthesis and the loss of *fliG1* only depleted the ability of the spirochete to swim in highly viscous media.

Flagella patterns (e.g. the number, length and cellular location of flagella) vary among different bacterial species (Aldridge and Hughes, 2002; Chevance and Hughes, 2008). For instance, *Vibrio cholera* has a single flagellum at one end of the cell, and *Pseudomonas aeruginosa* has a single flagellum at both ends. In contrast, enteric bacteria such as *E. coli* have multiple flagella that randomly locate on the cell surface. These patterns are essential for motility, e.g. alternations of number, location and length of flagella can either change swimming behaviours or totally disrupt motility (Klose and Mekalanos, 1998; Dasgupta *et al.*, 2000; Correa *et al.*, 2005; Murray and Kazmierczak, 2006). In this regard, the failure to

swim in highly viscous medium can be due to the alternation of flagellum pattern in the *fliG1*− mutant, e.g. the number, length and location of PFs. However, the electron microscopic analysis revealed that the *fliG1*− mutant shares the same pattern as the wild type with respect to the number, length and location of PFs (Fig. 4), implying the failure to swim in highly viscous medium is most likely caused by other factors such as flagellar motors.

Borrelia burgdorferi cells have two swimming behaviours: run and flex (Li *et al.*, 2002; Motaleb *et al.*, 2005; Bakker *et al.*, 2006). During run (translational motility), the two bundles of PFs have to be rotating asymmetrically: the leading end rotates counterclockwise (CCW), while the other end simultaneously rotates clockwise (CW). Cells would flex or tumble if both bundles of PFs rotate in the same direction. The leading end can switch from one end to the other when cells reverse (Video S3). Motion analysis demonstrated that the swimming behaviour of the *fliG1*− mutant is quite unique: one end of cells constantly gyrated and often switched direction, whereas the other end failed to gyrate (Video S4). The gyration is generated by the rotation of PFs, which is propelled by the flagellar motors. Thus, the failure of gyration is most likely caused by the dysfunction of the flagellar motors at the end with FliG1. Consistently, FliG1 was found to asymmetrically locate at one end of the cells. Previous studies indicate that both bundles of PFs rotate during the translational motility. Therefore, in the *fliG1*− mutant, the torque generated by one bundle of PFs may be insufficient to propel the cells to displace in highly viscous media such as 1% methylcellulose. However, the molecular mechanism involved still remains unknown. We are currently applying different approaches to elucidate the role of FliG1 in the flagellar motors. For example, cryo-EM has recently been applied to study *B. burgdorferi* cell and motor structures (Charon *et al.*, 2009; Liu *et al.*, 2009). This approach can be utilized to determine the location of FliG1 in the flagella motors. Co-immunoprecipitation and affinity blot analysis can be conducted to investigate the molecular partners of FliG1, e.g. the protein(s) that interacts with FliG1 (Toker and Macnab, 1997). The information obtained from these assays can help us to further disclose the molecular mechanism involved in the function of FliG1.

In enteric bacteria, flagella randomly locate on cell surface. Consistently, flagella motor switch complex proteins such as FliM and FliG appear as discrete spots along the sides of the cells (Sourjik and Berg, 2000). However, in spirochetes, two bundles of PFs are attached subterminally to the ends of the cells. Since the motors are associated with flagella, it is believed that flagella motor complex proteins locate at the cell poles (Charon and Goldstein, 2002; Li *et al.*, 2002). In this report, immunofluorescence analysis demonstrated that FliG2 locates at the two ends of the cells, which is consistent with the polar location of PFs in spirochete cells. In contrast to FliG2, the asymmetrical location of FliG1 is quite unique. Asymmetrical localization of specific proteins and structures have been discovered in several bacterial species (Shapiro and Losick, 2000; Lybarger and Maddock, 2001; Thanbichler and Shapiro, 2008). For instance, the stalk structure localizes at one end of the cell in *Caulobacter crescentus* at a site previously occupied by the flagellum. The ActA protein of *Listeria monocytogenes* and the IcsA protein of *Shigella flexneri* localize at one of the cell poles in each of these species, but the mechanisms involved in their asymmetric

localization are different. The localization of IcsA depends on direct targeting to a specific cell pole, whereas ActA is excluded from the newly synthesized cell pole. The asymmetrical localization of FliG1 can be achieved by one of these two mechanisms, e.g. FliG1 can be directly targeted to a new cell pole or be excluded from the new cell pole and consequently resides at the old cell pole.

Pathogenic spirochetes share some common pathogenic aspects, despite the fact that the clinical manifestations of the diseases caused by them are quite diverse (Norris *et al.*, 2001; Antal *et al.*, 2002; Steere *et al.*, 2004; Rosa *et al.*, 2005; LaFond and Lukehart, 2006; Palaniappan *et al.*, 2007; Vijayachari *et al.*, 2008). After encountering a mammalian host, microorganisms typically enter into the host either by ingress (e.g. inhalation and ingestion) or by penetration (e.g. insect bites, cuts and wounds on skin). For penetration, microorganisms have to cross epithelial barriers, enter into tissues, disseminate in hosts, and finally cause systemic infections. The spirochetes generally enter mammalian hosts by penetration after crossing epithelial barriers, which are mediated by either tick bite, sexual contact or through cuts and wounds on the skin. After being deposited on the skin or mucous membranes, these spirochetes must traverse the intercellular matrix, in some cases penetrate vascular endothelial cell lining, and finally spread in a host and cause systemic infections (Szczepanski *et al.*, 1990; Charon and Goldstein, 2002; Steere *et al.*, 2004; Palaniappan *et al.*, 2007). It has been believed that motility is essential for the invasion and dissemination of spirochetes (Kimsey and Spielman, 1990; Charon and Goldstein, 2002; Rosa *et al.*, 2005). However, the relevant evidence is quite limited.

Sadziene *et al.* (1991) isolated a non-flagella mutant of *B. burgdorferi* (HB19−) and found that this mutant failed to invade human tissues. However, HB19− is a spontaneous mutant and real mutation remains unknown. Botkin *et al*. constructed 33 *B. burgdorferi* mutants using transposon mutagenesis. Single mouse inoculations followed by culture of four tissue sites showed that three of these mutants were non-infectious, including a *fliG1* insertion mutant (Botkin *et al.*, 2006), which is consistent with this report. However, the phenotype of this mutant is not well characterized and the mutant is not complemented. In this communication, the phenotype of the *fliG1*− mutant is well characterized and the mutation was complemented. Thus, this mutant is a perfect candidate to determine whether motility is required for the infection of *B. burgdorferi*.

We first tested the *fliG1*− mutant in immunocompetent mice and found that the mutant failed to establish a systemic infection. In the process of *B. burgdorferi* infection, the spirochete is first deposited in mammalian skin tissue via tick bite and establishes a local infection. In this process, the spirochete has to escape from the innate immune responses, e.g. phagocytosis mediated by macrophages or neutrophils. It hypothesizes that motility facilitates the spirochete in traversing connective tissues, penetrating vascular endothelial cell linings and becoming haematogenous, and consequently helping spirochetes to escape the innate immune response (Greenberg and Canale-Parola, 1977a,b; Charon and Goldstein, 2002). Thus, the failure to establish a systemic infection in immunocompetent mice could be due to: the mutant fails to disseminate but retains the ability to establish local infection at inoculation sites; and/or the mutant can effectively evade innate immunity but is cleared by adaptive immune responses; and/or the mutant is simply eliminated by the innate immune

system immediately after inoculation. To address these possibilities, the mutant was further tested in SCID mice. The result showed that the mutant cells were cleared from all inoculation sites within 24 h, thus ruling out the possibility of the involvement of adaptive immunity in eliminating the mutant. The most likely mechanism could be that the inability to swim provides the innate immune system, including phagocytes, an opportunity. Consequently, non-motile spirochetes are quickly eliminated. Taken together, this report has demonstrated that motility is an important virulent factor that plays an essential role in spirochetal pathogenesis.

Experimental procedures

Bacterial strains and growth conditions

The high-passage *B. burgdorferi sensu stricto* strain B31A and the low-passage strain B31-A3 have been previously described (Elias *et al.*, 2002; Li *et al.*, 2002). Cells were grown at 34°C in BSK-II liquid or on plates in 3% carbon dioxide. Mutants derived from B31A or B31-A3 were grown in the presence of kanamycin (300 μg ml^{-1}), streptomycin (80 μg ml^{-1}) or gentamicin (40 μg ml^{-1}). *E. coli* JM109 and M15 cells were grown in Luria–Bertani broth with the appropriate antibiotic.

Construction of plasmids for the targeted mutagenesis

A previously described targeted mutagenesis that is mediated by allelic exchange recombination was applied to inactivate motility and chemotaxis genes in *B. burgdorferi* (Li *et al.*, 2002; Sal *et al.*, 2008; Yang and Li, 2009). Here, the *fliG1* was used as an example to describe how these mutants were constructed. As illustrated in Fig. 2, to construct a vector for targeted mutagenesis, the *fliG1* gene and a kanamycin resistance gene (*kan*) were amplified by PCR (primers P_1–P_4, Table 4), and the resultant PCR products were cloned into a pGEM-T vector (Promega, Madison, WI), and then *kan* was inserted into the *fliG1* gene at two HindIII sites, resulting in 346 bp deletion. The resultant plasmid was treated with NotI to linearize the plasmid, and the obtained product (approximately 5 μg) was electroporated into competent *B. burgdorferi* B31A cells. After 14–21 days of incubation, antibiotic-resistant colonies were picked and grown in BSK-II liquid medium for further analysis. The mutants were confirmed by PCR and the loss of cognate gene product was further detected by Western blot as previously described (Li *et al.*, 2002; Sal *et al.*, 2008; Yang and Li, 2009). The same strategy was used to construct the plasmids for the targeted mutagenesis of *fliG2*.

Complementation of the *fliG1*− and *fliG2*− mutants

The similar methods described before were used to complement the *fliG1*− mutant (Bakker *et al.*, 2006; Sal *et al.*, 2008). As shown in Fig. 2, the *flgB* promoter was first amplified by PCR with an engineered BamHI site at the 5′ end and an NdeI site at the 3′ end (primers were listed in Table 4). The intact *fliG1* gene was also amplified by PCR with engineered NdeI site at 5′ and SphI site at 3′ end. The resultant PCR fragments were cloned into the pGEM-T Easy vector. The *fliG1* gene was fused to the 3′ end of *flgB* promoter at the NdeI site, and confirmed by DNA sequence analysis. The BamHI–SphI-digested *flgB-fliG1* fragment was further cloned into pKFSS1 vector (Frank *et al.*, 2003; Bakker *et al.*, 2006),

which resulted in the complementing plasmid FlgBG1/ pKFSS1. The resultant construct was transformed into the mutant by electroporation as previously described (Bakker *et al.*, 2006; Sal *et al.*, 2008). The obtained transformants were characterized by PCR and Western blot as previously described (Bakker *et al.*, 2006; Motaleb *et al.*, 2007; Sal *et al.*, 2008). One complemented strain was selected for further studies and was named as *fliG1*$^{-/+}$. The similar method was applied to complement *fliG2*−. Although the complementation recovered the expression of *fliG2* (Fig. 3C), it could not restore the phenotype of the wild type. The obtained strain was referred to as *fliG2*$^{-/+}$.

Construction of the *fliG1* mutant and its complemented strain in B31-A3

To construct the *fliG1* mutant in the virulent strain B31-A3, the same construct described above was transformed into B31-A3 by electroporation. Cell plating and mutant screening were the same as the above. The plasmid profile in the obtained mutant was detected by PCR as previously described (Elias *et al.*, 2002; Stewart *et al.*, 2005). Only the mutant containing the same plasmid content as its parental strain B31-A3 was selected for the further characterization and the complementation. To complement the obtained *fliG1*−mutant, the above construct *flgB-fliG1* was cloned into the shuttle vector pBSV2G that contains gentamicin-resistant marker (Elias *et al.*, 2003; Grimm *et al.*, 2004). The resultant construct, FlgBG1/pBSV2G, was then transformed into the *fliG1*− mutant that was derived from B31-A3 as described before (Grimm *et al.*, 2004). The plasmid profile in the complemented strain was further confirmed by PCR analysis (Elias *et al.*, 2002). The obtained mutant and complemented strains on B31-A3 background were referred to as *vfliG1*−and *vfliG1*$^{-/+}$ respectively.

Generation of polyclonal antiserum against FliG1 or FliG2

The *fliG1* and *fliG2* genes were amplified using primers P_{15} to P_{18} (Table 4), and the PCR products were first cloned into the pGME-T Easy vector and the resulted insert was further subcloned into the pQE30 expression vector (Qiagen, Valencia, CA), which encodes an N-terminal histidine tag. The expression of *fliG1* and *fliG2* was induced using 0.1 M isopropyl-β-D-thiogalactoside (IPTG), and the recombinant proteins were purified by a nickel agarose column, and concentrated in 10 kDa molecular weight cut-off Amicon Ultra centrifugal concentrators (Millipore, Billerica, MA). Rats were immunized with 1 mg of purified recombinant proteins during a 1-month period. Polyclonal antisera were further purified by an affinity chromatography with the AminoLink Plus Immobilization Kit (Thermo Scientific, Rockford, IL), and eluted as recommended by the manufacturer.

Electrophoresis and Western blotting analysis

Sodium dodecyl sulphate-polyacrylamide gel electrophoresis (SDS-PAGE) and Western blotting using the enhanced chemiluminescent detection system (ECL) were performed as previously described (Li *et al.*, 2002; Sal *et al.*, 2008). All gels were 10% polyacrylamide unless otherwise noted. Whole cell lysates were prepared by first washing cells in PBS, followed by boiling for at least 5 min in Laemmli sample buffer. The antibodies against FliG1 or FliG2 were described above, and the antibodies against *B. burgdorferi* DnaK, FlaA

and FlaB were described in our previous studies (Sal *et al.*, 2008). Monoclonal antibody against GFP was purchased from Invitrogen (Carlsbad, California).

Swarm plate assay and bacterial tracking analysis

The motility of the above constructed mutants and complemented strains were analysed by a computer-based bacteria tracking system and swarm plate assay as previously described (Li *et al.*, 2002; Bakker *et al.*, 2006; Motaleb *et al.*, 2007). For bacterial tracking analysis, the strains were tracked under both a low viscous medium (BSK-II) and a highly viscous medium (1% methylcellulose). The swarm plate assay was performed on 1:10 diluted BSK-II medium containing 0.35% argarose.

Construction of a plasmid that expresses N-terminal GFP-fusion proteins

The same methods described before (with slight modification) were used to construct a vector that expresses N-terminal GFP-fusion protein (Sourjik and Berg, 2000). Figure 6A is the map of the vector expressing N-terminal GFP. The *gfp* gene was kindly provided by Dr Radolf's laboratory, which is driven by the *flgB* promoter (Eggers *et al.*, 2002). In this vector, a five-glycine linker was added between GFP and a fused protein, which allows GFP and the fused protein to fold independently and correctly (Sourjik and Berg, 2000). A unique restriction enzyme (SphI) cut site was engineered for the insertion of a fused gene, and a T7 terminator was added at the end of a fused gene. The final construct was named as pFBgfp/T7t. To express fusion protein GFP–FliG1, the full-length *fliG1* gene was PCR amplified with engineered SphI cut site at each end. The obtained PCR product was first cloned into pGEM-T easy vector and further subcloned into pFBgfp/T7t at the SphI site. The orientation of *fliG1* in this vector was further confirmed by restriction digestion and DNA sequencing. To localize GFP–FliG1 protein, the obtained plasmid was transformed into the *fliG1*− mutant by electroporation. The transformants were selected and confirmed as described above. The primers (P_{19} to P_{26}) for constructing this vector and GFP–FliG1 were enclosed in Table 4.

Light, fluorescence and electron microscopy

Cell morphology and motility of the wild type, *fliG1* mutant cells, as well as the complemented strains were characterized using light microscopy as previously described (Li *et al.*, 2002; Bakker *et al.*, 2006; Sal *et al.*, 2008). To visualize the motion of B31A and the *fliG1*− mutant, the cells in BSK-II medium were videotaped with dark-field illumination at 100× for at least 1 min. Video was digitized to allow for frame-by-frame observation of cell motion.

Immunofluorescence microscopic analysis was conducted to localize FliG2 as previously described (Hiraga *et al.*, 1998). Briefly, 1.5 ml of B31A and the *fliG2*− mutant cultures were harvested, washed two times with PBS buffer (phosphate-buffered saline, pH 7.5), and then treated with methanol at −20°C for 1 h. The collected cells were treated with lysozyme (1 mg ml^{-1}) in GTE buffer (50 mM glucose, 25 mM Tris, 1 mM EDTA, pH 7.5) for 1 h at room temperature, and then placed on a polysine-coated coverslip, allowed to fully dry in air. The obtained coverslips were first incubated in a blocking solution (2% BSA in PBS, pH 7.5) for 1 h, and then incubated in the blocking solution containing 1:500 diluted anti-FliG2

antibody for 1 h at room temperature. Finally, the coverslips were washed five times with PBS, incubated with secondary goat anti-rat Texas red antibody (Invitrogen) for 1 h at room temperature, washed with PBS again, and mounted in 40% glycerol for image process.

GFP images were taken using a Zeiss Axiostar *plus* microscope at a wave length of 480 nm. Texas red images were taken using a Zeiss Axioimager Z1 Axiophot wide-field microscope with an excitation filter (541–569) and an emission filter (581–654 nm). The images were captured and processed using the program Axiovision (Zeiss, Germany). To assay for the presence of PFs by electron microscopy, the wild-type and mutant cells were fixed, embedded, and observed by a JEOL JEM 1220 transmission electron microscopy as previously described (Li *et al.*, 2008; Sal *et al.*, 2008).

Infection studies in mice

Both BALB/c and BALB/c SCID mice at ages of 4–8 weeks (provided by the Division of Laboratory Animal Medicine at Louisiana State University) were used in the study as described previously (Xu *et al.*, 2005; 2008). All animal procedures were performed in compliance with the guidelines and with the approval of the Institutional Animal Care and Use Committee (IACUC). Briefly, BALB/c mice were given a single subcutaneous injection of 10^4 spirochetes, and sacrificed 4 weeks post inoculation. Heart, tibiotarsal joint and skin specimens were aseptically collected for spirochete culture. SCID mice received two intradermal/subcutaneous injections of 10^4 spirochetes. The two inoculation sites were at least 2 cm apart. Animals were sacrificed 24, 48 or 72 h later; inoculation site skin tissues were harvested for spirochete isolation.

Supplementary Material

Refer to Web version on PubMed Central for supplementary material.

Acknowledgments

We thank J. Radolf for providing *gfp* construct, S. Samuels and P. Rosa for providing the shuttle vectors and *B. burgdorferi* strains, N. Charon for sharing the computer-based bacteria tracking system, and the Confocal Microscope and Flow Cytometry Facility in the School of Medicine and Biomedical Sciences, University at Buffalo for the assistance of fluorescent microscope. This research was supported by Public Service AI073354, AI078958, and American Heart Association grants to C. Li, and AI29743 to N. Charon.

References

Aldridge P, Hughes KT. Regulation of flagellar assembly. Curr Opin Microbiol. 2002; 5:160–165. [PubMed: 11934612]

Antal GM, Lukehart SA, Meheus AZ. The endemic treponematoses. Microbes Infect. 2002; 4:83–94. [PubMed: 11825779]

Bakker RG, Li C, Miller MR, Cunningham C, Charon NW. Identification of specific chemoattractants and genetic complementation of a *Borrelia burgdorferi* chemotaxis mutant: a flow cytometry-based capillary tube chemotaxis assay. Appl Environ Microbiol. 2006; 73:1180–1188. [PubMed: 17172459]

Barthold SW. Animal models for Lyme disease. Lab Invest. 1995; 72:127–130. [PubMed: 7853847]

Berg HC, Turner L. Movement of microorganisms in viscous environments. Nature (London). 1979; 278:349–351. [PubMed: 370610]

Blevins JS, Revel AT, Smith AH, Bachlani GN, Norgard MV. Adaptation of a luciferase gene reporter and *lac* expression system to *Borrelia burgdorferi*. Appl Environ Microbiol. 2007; 73:1501–1513. [PubMed: 17220265]

Botkin DJ, Abbott A, Stewart PE, Rosa PA, Kawabata H, Watanabe H, Norris SJ. Identification of potential virulence determinants by *Himar1* transposition of infectious. Infect Immun. 2006; 74:6690–6699. [PubMed: 17015459]

Brown PN, Hill CP, Blair DF. Crystal structure of the middle and C-terminal domains of the flagellar rotor protein FliG. EMBO J. 2002; 21:3225–3234. [PubMed: 12093724]

Brown PD, Carrington DG, Gravekamp C, van de Kemp H, Edwards CN, Jones SR, et al. Direct detection of leptospiral material in human postmortem samples. Res Microbiol. 2003; 154:581–586. [PubMed: 14527659]

Charon NW, Goldstein SF. Genetics of motility and chemotaxis of a fascinating group of bacteria: the spirochetes. Annu Rev Genet. 2002; 36:47–73. [PubMed: 12429686]

Charon NW, Goldstein SF, Marko M, Hsieh C, Gebhardt LL, Motaleb MA, et al. The flat-ribbon configuration of the periplasmic flagella of *Borrelia burgdorferi* and its relationship to motility and morphology. J Bacteriol. 2009; 191:600–607. [PubMed: 19011030]

Chen ZQ, Zhang GC, Gong XD, Lin C, Gao X, Liang GJ, et al. Syphilis in China: results of a national surveillance programme. Lancet. 2007; 369:132–138. [PubMed: 17223476]

Chevance FF, Hughes KT. Coordinating assembly of a bacterial macromolecular machine. Nat Rev Microbiol. 2008; 6:455–465. [PubMed: 18483484]

Correa NE, Peng F, Klose KE. Roles of the regulatory proteins FlhF and FlhG in the *Vibrio cholerae* flagellar transcription hierarchy. J Bacteriol. 2005; 187:6324–6332. [PubMed: 16159765]

Dasgupta N, Arora SK, Ramphal R. *fleN*, a gene that regulates flagellar number in *Pseudomonas aeruginosa*. J Bacteriol. 2000; 182:357–364. [PubMed: 10629180]

Eggers CH, Caimano MJ, Clawson ML, Miller WG, Samuels DS, Radolf JD. Identification of loci critical for replication and compatibility of a *Borrelia burgdorferi* cp32 plasmid and use of a cp32-based shuttle vector for the expression of fluorescent reporters in the lyme disease spirochaete. Mol Microbiol. 2002; 43:281–295. [PubMed: 11985709]

Elias AF, Stewart PE, Grimm D, Caimano MJ, Eggers CH, Tilly K, et al. Clonal polymorphism of *Borrelia burgdorferi* strain B31 MI: implications for mutagenesis in an infectious strain background. Infect Immun. 2002; 70:2139–2150. [PubMed: 11895980]

Elias AF, Bono JL, Kupko JJ III, Stewart PE, Krum JG, Rosa PA. New antibiotic resistance cassettes suitable for genetic studies in *Borrelia burgdorferi*. J Mol Microbiol Biotechnol. 2003; 6:29–40. [PubMed: 14593251]

Frank KL, Bundle SF, Kresge ME, Eggers CH, Samuels DS. *aadA* confers streptomycin resistance in *Borrelia burgdorferi*. J Bacteriol. 2003; 185:6723–6727. [PubMed: 14594849]

Fraser CM, Casjens S, Huang WM, Sutton GG, Clayton R, Lathigra R, et al. Genomic sequence of a Lyme disease spirochaete, *Borrelia burgdorferi*. Nature. 1997; 390:580–586. [PubMed: 9403685]

Fraser CM, Norris SJ, Weinstock GM, White O, Sutton GG, Dodson R, et al. Complete genome sequence of *Treponema pallidum*, the syphilis spirochete. Science. 1998; 281:375–388. [PubMed: 9665876]

Goldstein SF, Charon NW, Kreiling JA. *Borrelia burgdorferi* swims with a planar waveform similar to that of eukaryotic flagella. Proc Natl Acad Sci USA. 1994; 91:3433–3437. [PubMed: 8159765]

Greenberg EP, Canale-Parola E. Motility of flagellated bacteria in viscous environments. J Bacteriol. 1977a; 132:356–358. [PubMed: 410784]

Greenberg EP, Canale-Parola E. Relationship between cell coiling and motility of spirochetes in viscous environments. J Bacteriol. 1977b; 131:960–969. [PubMed: 330506]

Grimm D, Tilly K, Byram R, Stewart PE, Krum JG, Bueschel DM, et al. Outer-surface protein C of the Lyme disease spirochete: a protein induced in ticks for infection of mammals. Proc Natl Acad Sci USA. 2004; 101:3142–3147. [PubMed: 14970347]

Hiraga S, Ichinose C, Niki H, Yamazoe M. Cell cycle-dependent duplication and bidirectional migration of SeqA-associated DNA–protein complexes in *E. coli*. Mol Cell. 1998; 1:381–387. [PubMed: 9660922]

Holt SC. Anatomy and chemistry of spirochetes. Microbiol Rev. 1978; 42:114–160. [PubMed: 379570]

Irikura VM, Kihara M, Yamaguchi S, Sockett H, Macnab RM. *Salmonella typhimurium fliG* and *fliN* mutations causing defects in assembly, rotation, and switching of the flagellar motor. J Bacteriol. 1993; 175:802–810. [PubMed: 8423152]

Kimsey RB, Spielman A. Motility of Lyme disease spirochetes in fluids as viscous as the extracellular matrix. J Infect Dis. 1990; 162:1205–1208. [PubMed: 2230247]

Klose KE, Mekalanos JJ. Differential regulation of multiple flagellins in *Vibrio cholerae*. J Bacteriol. 1998; 180:303–316. [PubMed: 9440520]

Kuiper H, van Dam AP, Spanjaard L, de Jongh BM, Widjojokusumo A, Ramselaar TC, et al. Isolation of *Borrelia burgdorferi* from biopsy specimens taken from healthy-looking skin of patients with Lyme borreliosis. J Clin Microbiol. 1994; 32:715–720. [PubMed: 8195384]

LaFond RE, Lukehart SA. Biological basis for syphilis. Clin Microbiol Rev. 2006; 19:29–49. [PubMed: 16418521]

Leadbetter JR, Schmidt TM, Graber JR, Breznak JA. Acetogenesis from H_2 plus CO_2 by spirochetes from termite guts. Science. 1999; 283:686–689. [PubMed: 9924028]

Levett PN. Leptospirosis. Clin Microbiol Rev. 2001; 14:296–326. [PubMed: 11292640]

Li C, Motaleb A, Sal M, Goldstein SF, Charon NW. Spirochete periplasmic flagella and motility. J Mol Microbiol Biotechnol. 2000; 2:345–354. [PubMed: 11075905]

Li C, Bakker RG, Motaleb MA, Sartakova ML, Cabello FC, Charon NW. Asymmetrical flagellar rotation in *Borrelia burgdorferi* nonchemotactic mutants. Proc Natl Acad Sci USA. 2002; 99:6169–6174. [PubMed: 11983908]

Li C, Wolgemuth CW, Marko M, Morgan DG, Charon NW. Genetic analysis of spirochete flagellin proteins and their involvement in motility, filament assembly, and flagellar morphology. J Bacteriol. 2008; 190:5607–5615. [PubMed: 18556797]

Liu J, Lin T, Botkin DJ, McCrum E, Winkler H, Norris SJ. Intact flagellar motor of *Borrelia burgdorferi* revealed by cryo-electron tomography: evidence for stator ring curvature and rotor/C ring assembly flexion. J Bacteriol. 2009; 191:5026–5036. [PubMed: 19429612]

Lloyd SA, Tang H, Wang X, Billings S, Blair DF. Torque generation in the flagellar motor of *Escherichia coli*: evidence of a direct role for FliG but not for FliM or FliN. J Bacteriol. 1996; 178:223–231. [PubMed: 8550421]

Lloyd SA, Whitby FG, Blair DF, Hill CP. Structure of the C-terminal domain of FliG, a component of the rotor in the bacterial flagellar motor. Nature. 1999; 400:472–475. [PubMed: 10440379]

Lux R, Moter A, Shi W. Chemotaxis in pathogenic spirochetes: directed movement toward targeting tissues? J Mol Microbiol Biotechnol. 2000; 2:355–364. [PubMed: 11075906]

Lybarger SR, Maddock JR. Polarity in action: asymmetric protein localization in bacteria. J Bacteriol. 2001; 183:3261–3267. [PubMed: 11344132]

McBride AJ, Athanazio DA, Reis MG, Ko AI. Leptospirosis. Curr Opin Infect Dis. 2005; 18:376–386. [PubMed: 16148523]

Masuzawa T, Beppu Y, Kawabata H, Yanagihara Y, Iwamoto Y, Shimizu T, Johnson RC. Experimental *Borrelia burgdorferi* infection of outbred mice. J Clin Microbiol. 1992; 30:3016–3018. [PubMed: 1452675]

Mikosza AS, Hampson DJ. Human intestinal spirochetosis: *Brachyspira aalborgi* and/or *Brachyspira pilosicoli*? Anim Health Res Rev. 2001; 2:101–110. [PubMed: 11708739]

Motaleb MA, Corum L, Bono JL, Elias AF, Rosa P, Samuels DS, Charon NW. *Borrelia burgdorferi* periplasmic flagella have both skeletal and motility functions. Proc Natl Acad Sci USA. 2000; 97:10899–10904. [PubMed: 10995478]

Motaleb MA, Miller MR, Li C, Bakker RG, Goldstein SF, Silversmith RE, et al. CheX is a phosphorylated CheY phosphatase essential for *Borrelia burgdorferi* chemotaxis. J Bacteriol. 2005; 187:7963–7969. [PubMed: 16291669]

Motaleb MA, Miller MR, Bakker RG, Li C, Charon NW. Isolation and characterization of chemotaxis mutants of the Lyme disease spirochete *Borrelia burgdorferi* using allelic exchange mutagenesis, flow cytometry, and cell tracking. Methods Enzymol. 2007; 422:419–437.

Murray TS, Kazmierczak BI. FlhF is required for swimming and swarming in *Pseudomonas aeruginosa*. J Bacteriol. 2006; 188:6995–7004. [PubMed: 16980502]

Nocton JJ, Bloom BJ, Rutledge BJ, Persing DH, Logigian EL, Schmid CH, Steere AC. Detection of *Borrelia burgdorferi* DNA by polymerase chain reaction in cerebrospinal fluid in Lyme neuroborreliosis. J Infect Dis. 1996; 174:623–627. [PubMed: 8769624]

Norris SJ, Cox DL, Weinstock GM. Biology of *Treponema pallidum*: correlation of functional activities with genome sequence data. J Mol Microbiol Biotechnol. 2001; 3:37–62. [PubMed: 11200228]

Palaniappan RU, Ramanujam S, Chang YF. Leptospirosis: pathogenesis, immunity, and diagnosis. Curr Opin Infect Dis. 2007; 20:284–292. [PubMed: 17471039]

Paster BJ, Dewhirst FE. Phylogenetic foundation of spirochetes. J Mol Microbiol Biotechnol. 2000; 2:341–344. [PubMed: 11075904]

Ren SX, Fu G, Jiang XG, Zeng R, Miao YG, Xu H, et al. Unique physiological and pathogenic features of *Leptospira interrogans* revealed by whole-genome sequencing. Nature. 2003; 422:888–893. [PubMed: 12712204]

Rosa PA, Tilly K, Stewart PE. The burgeoning molecular genetics of the Lyme disease spirochaete. Nat Rev Microbiol. 2005; 3:129–143. [PubMed: 15685224]

Ruby JD, Charon NW. Effect of temperature and viscosity on the motility of the spirochete *Treponema denticola*. FEMS Microbiol Lett. 1998; 169:251–254. [PubMed: 9868769]

Sadziene A, Thomas DD, Bundoc VG, Holt SC, Barbour AG. A flagella-less mutant of *Borrelia burgdorferi*. Structural, molecular, and *in vitro* functional characterization. J Clin Invest. 1991; 88:82–92. [PubMed: 2056133]

Sal MS, Li C, Motalab MA, Shibata S, Aizawa S, Charon NW. *Borrelia burgdorferi* uniquely regulates its motility genes and has an intricate flagellar hook-basal body structure. J Bacteriol. 2008; 190:1912–1921. [PubMed: 18192386]

Samuels DS. Electrotransformation of the spirochete *Borrelia burgdorferi*. Methods Mol Biol. 1995; 47:253–259. [PubMed: 7550741]

Samuels DS, Mach KE, Garon CF. Genetic transformation of the Lyme disease agent *Borrelia burgdorferi* with coumarin-resistant *gyrB*. J Bacteriol. 1994; 176:6045–6049. [PubMed: 7928965]

Seshadri R, Myers GS, Tettelin H, Eisen JA, Heidelberg JF, Dodson RJ, et al. Comparison of the genome of the oral pathogen *Treponema denticola* with other spirochete genomes. Proc Natl Acad Sci USA. 2004; 101:5646–5651. [PubMed: 15064399]

Shapiro L, Losick R. Dynamic spatial regulation in the bacterial cell. Cell. 2000; 100:89–98. [PubMed: 10647934]

Sourjik V, Berg HC. Localization of components of the chemotaxis machinery of *Escherichia coli* using fluorescent protein fusions. Mol Microbiol. 2000; 37:740–751. [PubMed: 10972797]

Stanek G, Klein J, Bittner R, Glogar D. Isolation of *Borrelia burgdorferi* from the myocardium of a patient with longstanding cardiomyopathy. N Engl J Med. 1990; 322:249–252. [PubMed: 2294450]

Steere AC, Coburn J, Glickstein L. The emergence of Lyme disease. J Clin Invest. 2004; 113:1093–1101. [PubMed: 15085185]

Stewart PE, Hoff J, Fischer E, Krum JG, Rosa PA. Genome-wide transposon mutagenesis of *Borrelia burgdorferi* for identification of phenotypic mutants. Appl Environ Microbiol. 2004; 70:5973–5979. [PubMed: 15466540]

Stewart PE, Byram R, Grimm D, Tilly K, Rosa PA. The plasmids of *Borrelia burgdorferi*: essential genetic elements of a pathogen. Plasmid. 2005; 53:1–13. [PubMed: 15631949]

Szczepanski A, Furie MB, Benach JL, Lane BP, Fleit HB. Interaction between *Borrelia burgdorferi* and endothelium *in vitro*. J Clin Invest. 1990; 85:1637–1647. [PubMed: 2332509]

Thanbichler M, Shapiro L. Getting organized –how bacterial cells move proteins and DNA. Nat Rev Microbiol. 2008; 6:28–40. [PubMed: 18059290]

Toker AS, Macnab RM. Distinct regions of bacterial flagellar switch protein FliM interact with FliG, FliN and CheY. J Mol Biol. 1997; 273:623–634. [PubMed: 9356251]

Vijayachari P, Sugunan AP, Shriram AN. Leptospirosis: an emerging global public health problem. J Biosci. 2008; 33:557–569. [PubMed: 19208981]

Warnecke F, Luginbuhl P, Ivanova N, Ghassemian M, Richardson TH, Stege JT, et al. Metagenomic and functional analysis of hindgut microbiota of a wood-feeding higher termite. Nature. 2007; 450:560–565. [PubMed: 18033299]

Weinstock GM, Hardham JM, McLeod MP, Sodergren EJ, Norris SJ. The genome of *Treponema pallidum*: new light on the agent of syphilis. FEMS Microbiol Rev. 1998; 22:323–332. [PubMed: 9862125]

Xu Q, Seemanapalli SV, Lomax L, McShan K, Li X, Fikrig E, Liang FT. Association of linear plasmid 28-1 with an arthritic phenotype of *Borrelia burgdorferi*. Infect Immun. 2005; 73:7208–7215. [PubMed: 16239515]

Xu Q, McShan K, Liang FT. Essential protective role attributed to the surface lipoproteins of *Borrelia burgdorferi* against innate defences. Mol Microbiol. 2008; 69:15–29. [PubMed: 18452586]

Yang Y, Li C. Transcription and genetic analyses of a putative *N*-acetylmuramyl-L-alanine amidase in *Borrelia burgdorferi*. FEMS Microbiol Lett. 2009; 290:164–173. [PubMed: 19025570]

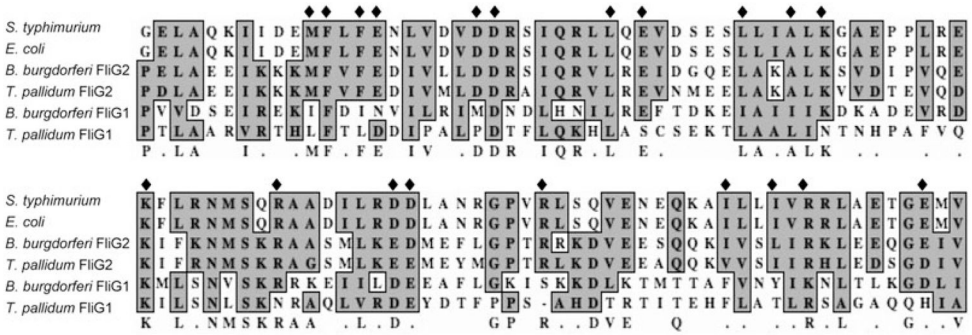

Fig. 1.

Multiple sequence alignment of the C-terminus of FliG proteins. The numbers show the positions of amino acids of *E. coli* and *Salmonella typhimurium* FliG proteins, and diamonds represent the key residues required for the function and structure of FliG proteins. GenBank accession numbers for the aligned proteins are: *S. typhimurium* FliG (NP_456531), *E. coli* FliG (NP_310705), *B. burgdorferi* FliG2 (NP_212424), *T. pallidum* FliG2 (NP_218840), *Bacillus subtilis* FliG (NP_389504), *B. burgdorferi* FliG1 (ZP_03086805) and *T. pallidum* FliG1 (NP_218466). The alignments were performed using the program MacVector 10.6.

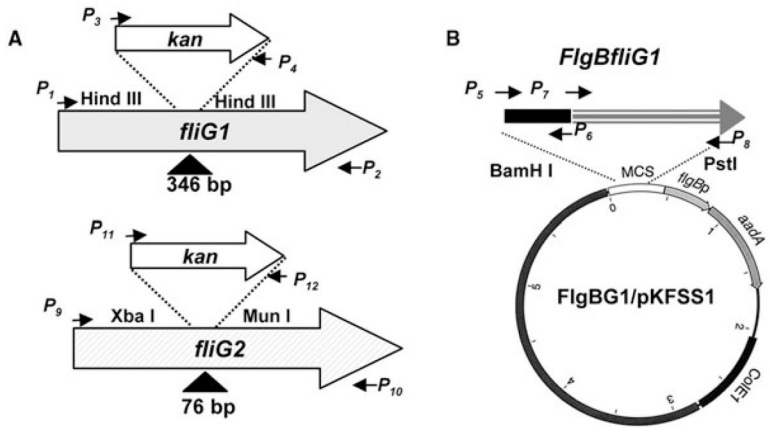

Fig. 2. Constructing plasmids for the inactivation of *fliG1* and *fliG2* genes and the complementation of *fliG1*− mutant

A. The constructs to inactivate *fliG1* and *fliG2* genes.

B. The plasmid FlgBG1/pKFSS1 was used to complement the *fliG1*− mutant *in trans*. Arrows indicate the relative positions of PCR primers for constructing these plasmids, and the sequences of these primers were listed in Table 4; the symbols ‘Δ’ show the DNA fragments deleted from the genes, and the numbers are the sizes of deleted DNA fragments.

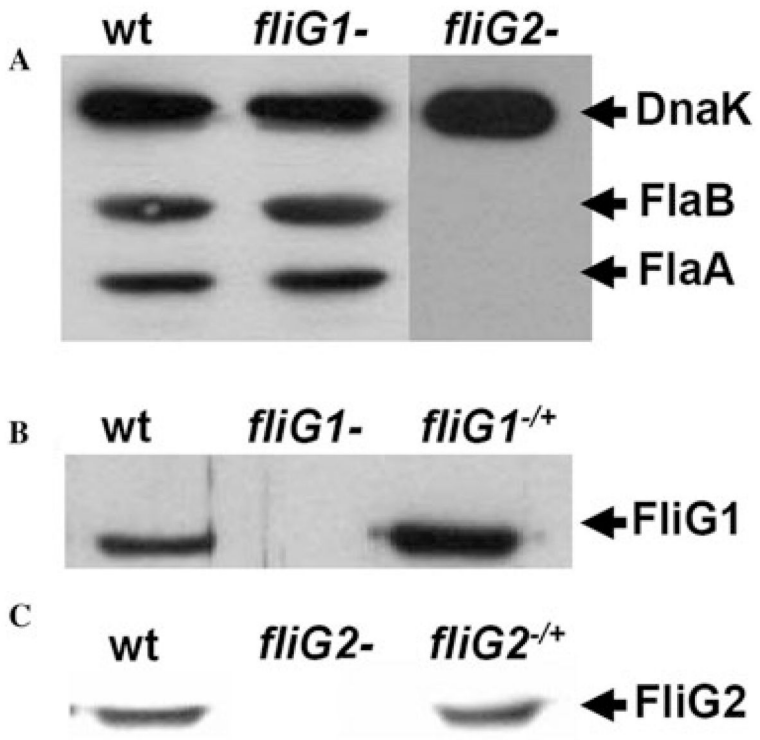

Fig. 3. Western blot analysis of the *fliG* mutants and their complemented strains

A. Flagella filament protein FlaA and FlaB are absent in the *fliG2*−mutant, but still present in the *fliG1*− mutant.

B and C. The cognate gene products were absent in the respective mutants and were restored in the complemented strains.

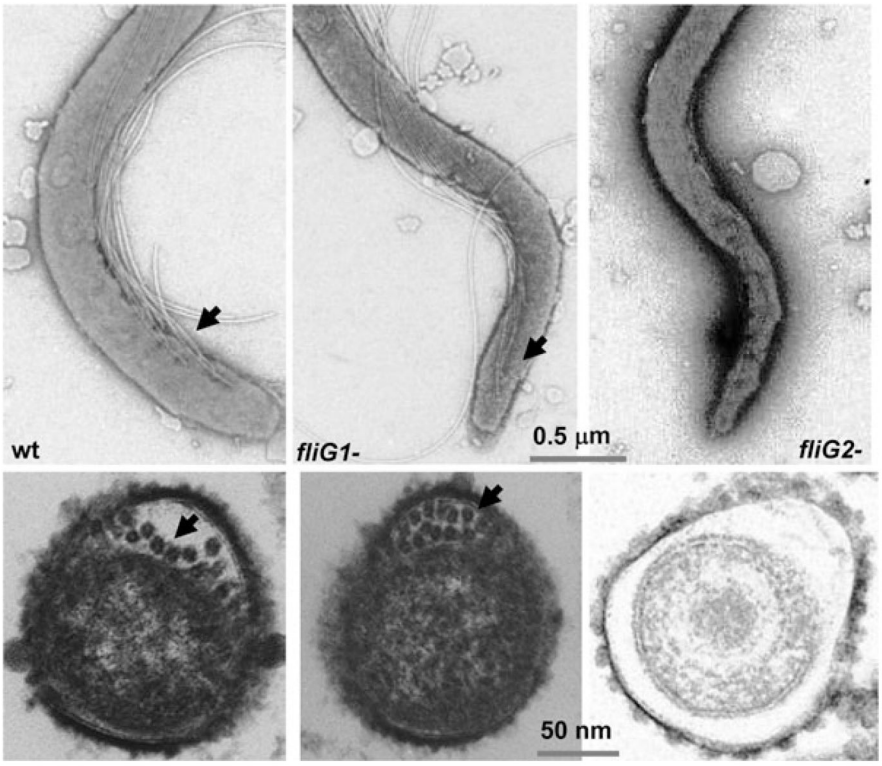

Fig. 4.

Electron microscopic analyses of the *fliG1*− and the *fliG2*− mutants. The upper panels are the electron micrographs of outer membrane-disrupted *B. burgdorferi* cells, and only one end of the cells was illustrated; the lower panel is the thin-section electron micrographs of *B. burgdorferi* cells. Arrows point to the PFs.

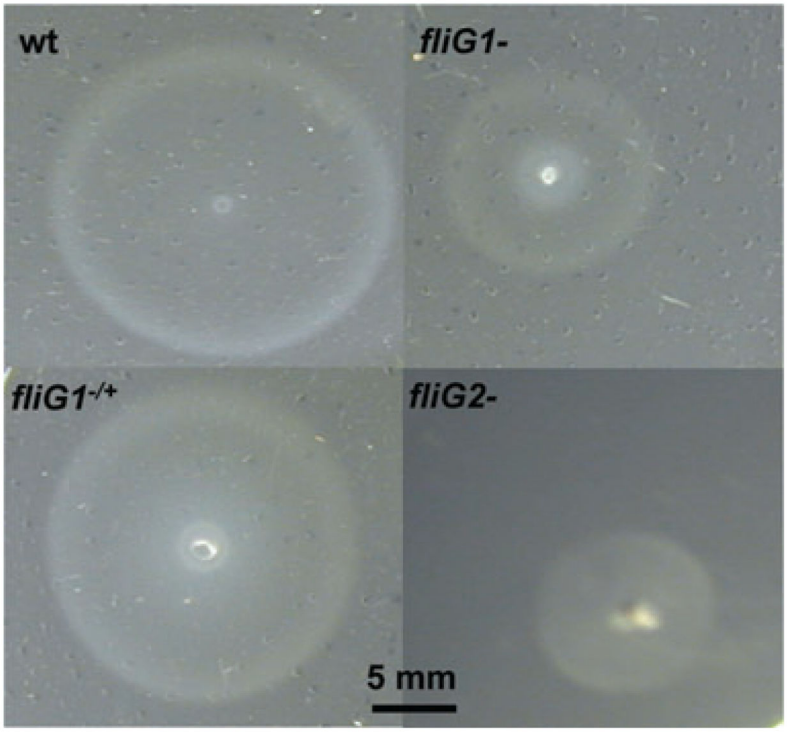

Fig. 5.

Swarm plate assays. The swarm plate assays were carried out on 0.35% agarose with 1:10 diluted BSK-II medium as previously described (Li *et al.*, 2002; Sal *et al.*, 2008). Diameters of swarms (centimetres) after 72 h of incubation: wild-type 2.1; *fliG1*−, 1.2; *fliG1*$^{-/+}$, 2.0; *fliG2*−, 0.9.

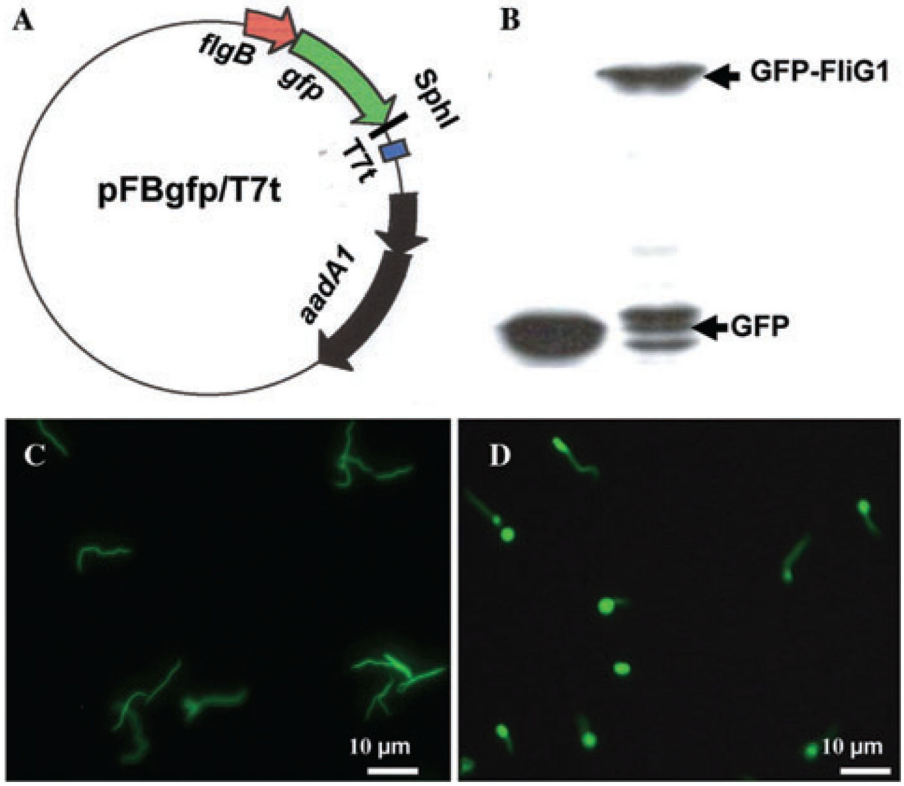

Fig. 6. Localization of FliG1 in *B. burgdorferi*

A. Constructing a vector that expresses the N-terminal GFP-fusion proteins. The *flgB* promoter element was fused to *gfp* with a five-glycine linker, and SphI cloning site was engineered at the 3′ end of *gfp*. A target gene, such as *fliG1*, will be fused to *gfp* at the SphI site. A T7 transcription terminator was inserted.

B. Detection of GFP–FliG1 fusion protein using Western blot. A monoclonal antibody against GFP (Invitrogen) was used to detect GFP and GFP–FliG1. GFP is about 27 kDa and GFP–FliG1 is about 75 kDa.

C. The fluorescence micrograph (40×) of the *fliG1* mutant that was transformed with the plasmid pFBgfp/T7t, which only expresses GFP.

D. The fluorescence micrograph (40×) of the *fliG1* mutant that was transformed with the plasmid pFBgfp–fliG1/T7t, which expresses GFP–FliG1 fusion protein. The brighter ends represent the location of GFP–FliG1.

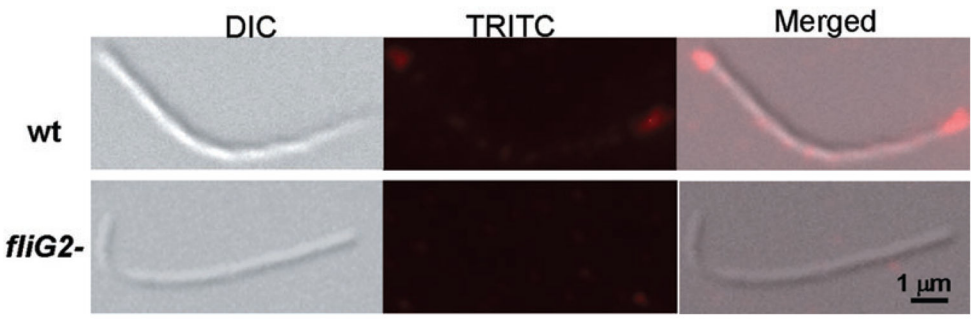

Fig. 7.

Localization of FliG2 in *B. burgdorferi* by immunofluorescence microscopy. The wild-type and the *fliG2*− mutant cells were fixed with methanol, stained with anti-FliG2 and counterstained with anti-rat Texas red-coupled antibody, as described in *Experimental procedures*. Photo (DIC) and fluorescent (TRITC) micrographs (100×) were, respectively, taken under a Zeiss Axioimager Z1 Axiophot microscope, and merged. For each strain, more than 50 cells were examined.

Table 1

Measuring the velocity of *B. burgdorferi* strains.

	Velocity (μm s^{-1})	
Strains	**BSK-II**	**1% methylcellulose**
B31A	Motile[a]	10.2 ± 2.2
fliG1−	Motile	No translational motility
fliG1$^{-/+}$	Motile	9.3 ± 3.9
fliG2−	Non-motile	Non-motile

[a] Velocity is less than 1 μm s^{-1}. The numbers are the average velocity calculated from at least 20 cells.

Table 2

The *vfliG1*− mutant was unable to infect mice.[a]

	No. of cultures positive/Total no. of specimens examined			
Clone	**Heart**	**Joint**	**Skin**	**All sites**
B31-A3	5/5	5/5	5/5	15/15
vfliG1 $^{-/+}$	5/5	5/5	5/5	15/15
vfliG1−	0/5	0/5	0/5	0/15

[a]Groups of five BALB/c mice were inoculated with 10^4 spirochetes of the B31-A3, *vfliG1*$^{-/+}$ or *vfliG1*− strains. Mice were sacrificed 4 weeks post inoculation; heart, tibiotarsal joint and skin specimens were harvested for spirochete culture in BSK-II medium.

Table 3

The *vfliG1*− mutant was quickly cleared from murine skin.[a]

	No. of sites positive/Total no. of sites examined at post-inoculation hours		
Clone	**24 h**	**48 h**	**72 h**
B31-A3	6/6	6/6	6/6
vfliG1$^{-/+}$	6/6	6/6	6/6
vfliG1−	0/6	0/6	0/6

[a]Groups of nine SCID mice each received two intradermal/ subcutaneous injections of the B31-A3, *vfliG1*$^{-/+}$ or *vfliG1*− strains. Approximately 10^4 organisms were administered in each inoculation; two inoculation sites were at least 2 cm apart. Three animals from each group were euthanized at 24, 48 and 72 h post inoculation; skin specimens were harvested from inoculation sites and cultured for spirochetes in BSK-II medium.

Table 4

Oligonucelotide primers used in this study.

Primer	Description	Sequences
P_1	*fliG1* (F), inactivation	5′-AGATTCAAGGCTCTATGC-3′
P_2	*fliG1* (R), inactivation	5′-TTTAGCAGTCTCTGTATCG-3′
P_3	*kan* (F), *fliG1* inactivation	5′-AAGCTTTAATACCCGAGCTTCAAG-3′
P_4	*kan* (R), *fliG1* inactivation	5′-AAGCTTTCAAGTCAGCGTAATGCT-3′
P_5	*flgBp* (F), complementation	5′-GGATCCTAATACCCGAGCTTCAAG-3′
P_6	*flgBp* (R), complementation	5′-CATATGACCTCCCTCATTTAAAATTGC-3′
P_7	*fliG1* (F), complementation	5′-CATATGAAAGTTATGCAGGATCCTAGG-3′
P_8	*fliG1* (R), complementation	5′-GCATGCGTGTCATTAAATAAATTCCTC-3′
P_9	*fliG2* (F), inactivation	5′-ATTCTGGATGTTTCTGCT-3′
P_{10}	*fliG2* (R), inactivation	5′-GACAAGCACATCTTCTTC-3′
P_{11}	*kan* (F), *fliG2* inactivation	5′-TCTAGATAATACCCGAGCTTCAAG-3′
P_{12}	*kan* (R), *fliG2* inactivation	5′-CAATTGTCAAGTCAGCGTAATGCT-3′
P_{13}	*fliG2* (F), complementation	5′-CATATGGAAGAAAAAAAAGAAAAGC-3′
P_{14}	*fliG2* (R), complementation	5′-GCATGCGACAAGCACATCTTCTTC-3′
P_{15}	*fliG1* (F), His-tagged FliG1	5′-GAGCTCGATCCTAGGCTTTCCAAGTAT-3′
P_{16}	*fliG1* (R), His-tagged FliG1	5′-CTGCAGTTTTTCTATATATTATTAAATCG-3′
P_{17}	*fliG2* (F), His-tagged FliG2	5′-GGATCCATTCTGGATGTTTCTGCT-3′
P_{18}	*fliG2* (R), His-tagged FliG2	5′-CTGCAGGACAAGCACATCTTCTTC-3′
P_{19}	*flgBp* (F), expressing *gfp*	5′-CTGCAGTAATACCCGAGCTTCAAG-3′
P_{20}	*flgBp* (R), expressing *gfp*	5′-GGATCCTTTAAAATTGCTTTTAAC-3′
P_{21}	*gfp* (F)	5′-GGATCCAAGAAGGAGATATACATATGAG-3′
P_{22}	*gfp* (R), with 5 × glycin linker	5′-GCATGCACCTCCACCTCCACCTTTGTATAGTTCATCCATGCCATGTG-3′
P_{23}	T7 terminator (F)	5′-GCATGCTAACAAAGCCCGAAAGGAAGC-3′
P_{24}	T7 terminator (R)	5′-AAGCTTGCAGATCCGGATATAGTTCCT-3′
P_{25}	*fliG1* (F), GFP fusion	5′-GCATGCAAAGTTATGCAGGATCCTAGGCTT-3′
P_{26}	*fliG1* (R), GFP fusion	5′-GCATGCGTGTCATTAAATAAATTCCTC-3′